A LETTERS JOURNAL EXPLORING THE FRONTIERS OF PHYSICS

Società Italiana di Fisica

sciences

IOP Institute of Physics

LETTER

Transformation of a submerged flat jet under strong transverse magnetic field

To cite this article: D. Krasnov *et al* 2021 *EPL* **134** 24003

A Letters Journal Exploring
the Frontiers of Physics

April 2021

EPL, **134** (2021) 24003
www.epljournal.org
doi: 10.1209/0295-5075/134/24003

Transformation of a submerged flat jet under strong transverse magnetic field

D. Krasnov[1(a)], Ya. Listratov[2,3], Yu. Kolesnikov[1], I. Belyaev[2,3], N. Pyatnitskaya[2,3], E. Sviridov[2] and O. Zikanov[4]

[1] *Technische Universität Ilmenau - PF 100565, 98684 Ilmenau, Germany*
[2] *Moscow Power Engineering Institute - Krasnokazarmennaya 14, 111250, Moscow, Russia*
[3] *Joint Institute for High Temperature RAS - Izhorskaya 13 Bd.2, 125412, Moscow, Russia*
[4] *University of Michigan-Dearborn - Dearborn, 48128-1491, MI, USA*

received 5 November 2020; accepted in final form 1 February 2021
published online 8 July 2021

Abstract – A duct flow generated by a planar jet at the inlet and affected by a magnetic field perpendicular to the jet's plane is analyzed in high-resolution numerical simulations. The case of very high Reynolds and Hartmann numbers is considered. It is found that the flow structure is drastically modified in the inlet area. It becomes determined by three new planar jets oriented along the magnetic field lines: two near the walls and one in the middle of the duct. The downstream evolution of the flow includes the Kelvin-Helmholtz instability of the jets and slow decay of the resulting quasi-two-dimensional turbulence.

Introduction. – Wall bounded shear flows of electrically conducting fluids subjected to static magnetic fields are found in many technological applications. The magnetic field transforms the flow in a way, which depends on the field's strength and orientation and may include complete restructuring of the mean velocity and modification of turbulence properties. The transformation is particularly radical when the magnetic field crosses the mean flow in the direction of its shear. An interesting type of such a situation is a submerged jet injected into a wall-bounded domain. The flow is also practically relevant. Such jets appear in molds of continuous steel casters or in elements of liquid metal blankets of nuclear fusion reactors.

The transformation of a submerged jet by a transverse magnetic field at high Reynolds and Hartmann numbers Re and Ha (defined below) is one of the classical problems of magnetohydrodynamics of liquid metals [1–4]. A key aspect of the transformation common for all flows with the magnetic field effect is the anisotropic suppression of velocity fluctuations by the Joule dissipation of the induced electric currents [5]. The main results of the suppression have been well documented as the damping of turbulence and 3D hydrodynamic instabilities, and, in flows with strong field effect, formation of quasi-two-dimensional (Q2D) structures, in which velocity has nearly zero gradients outside of thin Hartmann boundary layers (see, *e.g.*, [6–11]). Another major aspect is the interaction between the mean flow and the magnetic field. Its manifestations are case specific and determined by the flow and field orientations, location and electric conductivity of walls, and other features of the flow configuration.

Expansion of a round jet into an infinite domain was analyzed in [4]. It was argued that the conservation of linear momentum in the course of the magnetic damping implies existence of a lower bound of kinetic energy and, thus, requires that the flow acquires the form minimizing the Joule dissipation. The transformation was predicted to lead to reverse flow regions on the sides of the jet and its anisotropic expansion with the size in the field direction growing as $\sim x^{2/3}$. Partial experimental and computational validations of the scenario can be found in [12,13].

The jet transformation in a finite domain is, evidently, very different [1–3]. One illustration is the flow in a diverging duct [2], where a classical M-shaped velocity profile is formed, such that most of the flow rate is carried by planar jets located near the walls parallel to the magnetic field (the sidewalls). The typical velocity magnitudes in these layers and in the core are related to the average streamwise velocity as $\sim Ha^{1/2}$ and $\sim Ha^{-1/2}$, respectively. One should also mention the experimental [14] and numerical [15,16] works, where a sudden expansion into a duct

(a) E-mail: dmitry.krasnov@tu-ilmenau.de (corresponding author)

with a perpendicular magnetic field was studied. Flow regimes with separation zones and characteristic distributions of pressure and electric potential were identified. The geometry of [14–16] is analogous to that considered in our study, but the small expansion ratio (4:1), which makes the system more similar to a transition between two ducts, and the focus on steady-state stable flow regimes at moderate Re imply a quite different flow behavior.

Sudden expansion of a thin flat jet into a duct was studied in the classical experiments [1,3]. In [3], the transverse magnetic field was in the plane of the jet. This resulted in the suppression of jet's 3D instabilities and preservation of its near two-dimensionality at a distance greater than in the absence of the field. The two-dimensional instabilities caused by the strong shear and inflection points in the velocity profile were not suppressed. Their growth led to strong (about 60% relative to the mean velocity) Q2D perturbations and the properties of the velocity signal typical for nearly two-dimensional turbulence.

Our work is a direct continuation of [1], where the effect of the magnetic field perpendicular to the jet's plane was studied for the case of a jet with the expansion ratio 20:1 at $Re \leq 11600$, $Ha \leq 296$. Unfortunately, the data obtained in [1] were limited to the Pitot-Prandtl tube measurements of mean velocity. One important and verifiable result was the discovery of the flow's transformation into the form with an M-shaped velocity profile, *i.e.*, degeneration of the inlet jet and formation of two flat jets aligned with the field lines and located near the sidewalls. Increased velocity in the core region was also detected in some flow regimes, but the phenomenon did not receive any further attention.

Transformation of a thin flat jet expanding into a square duct in the presence of a strong magnetic field perpendicular to the jet's plane (see fig. 1) is studied in our work. A drastic modification of the flow is anticipated on the basis of the earlier studies, but the details of the transformation have, so far, remained practically unexplored. The study is conducted as a collaboration of numerical and experimental efforts. The preliminary data and outline of the methodology of the experiments can be found in [17]. This letter reports the first results of high-resolution numerical simulations.

Procedure and parameters. – We consider a flow of an incompressible electrically conducting fluid (*e.g.*, a liquid metal) in a square duct subjected to a uniform constant magnetic field $\boldsymbol{B}$ applied in the wall-normal direction z (see fig. 1). The inlet has the form of a rectangular gap located at the mid-plane $z = 0$ (see fig. 1). The gap extends over the entire duct width in the y-direction and has the width equal to 1/10th of the duct width in the z-direction.

The electromagnetic effects are described using the quasi-static approximation valid at small magnetic Reynolds and Prandtl numbers (the situation applicable to the majority of industrial and laboratory flows of liquid

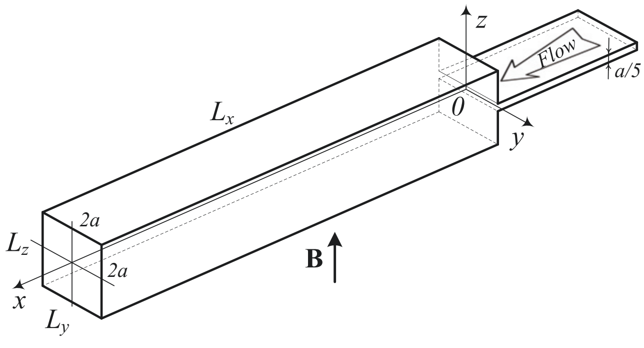

Fig. 1: Schematic representation of the flow.

metals [18]). The governing equations are written in terms of the velocity $\boldsymbol{u}$, pressure p, and electric potential ϕ. The flow is characterized by two dimensionless parameters: the Reynolds number $Re = U_q a/\nu$ and the Hartmann number $Ha = Ba(\sigma/\rho\nu)^{1/2}$. Here U_q is the mean velocity in the duct, a is the duct's half-width and ν, ρ, σ are the kinematic viscosity, density and electric conductivity.

The walls are assumed to be no-slip and perfectly electrically insulating. A velocity profile that mimics a laminar duct flow is prescribed in the gap. In order to check the effect of inlet disturbances on the flow, additional simulations were performed with random noise of non-dimensional amplitudes of 10^{-3} and 10^{-2} added to the inlet velocity. The flow behavior was found to be largely insensitive to the noise, so the results reported below are from the zero noise simulations. The convective outflow condition $\partial \boldsymbol{u}/\partial t + \partial \boldsymbol{u}/\partial x = 0$ is applied at the exit. The boundary conditions on the electric potential are $\partial\phi/\partial n = 0$ at the walls and $\partial\phi/\partial x = 0$ at the inlet and exit.

The problem is solved using a finite-difference scheme of the second order on a structured colocated grid [19]. The scheme is conservative for momentum, mass and electric charge and nearly conservative for the kinetic energy. The accuracy and efficiency of the scheme in simulations of high-Ha parallel shear flows has been demonstrated, *e.g.*, in [8,9,20]. The most recent version of the solver optimized for spatially evolving flows [21] is used in the present study.

The simulations are conducted in the domain $L_x \times L_y \times L_z = 8\pi \times 2 \times 2$ (see fig. 1) on a computational grid of $4096 \times 512 \times 512$ points. The grid is uniform in the x-direction and non-uniform in the y- and z-directions. In order to resolve thin MHD boundary layers, which is particularly important for MHD flows at high Ha, the grid is clustered towards the walls according to the modified Gauss-Lobatto coordinate transformation (shown for z)

$$z = 0.9\frac{L_z}{2}\sin\left(\frac{\pi}{2}\frac{\sinh(\zeta)}{\sinh(1)}\right) + 0.1\zeta,$$

where $-1 \leq \zeta \leq 1$ is the transformed coordinate, in which the grid is uniform. This transformation is preferable to

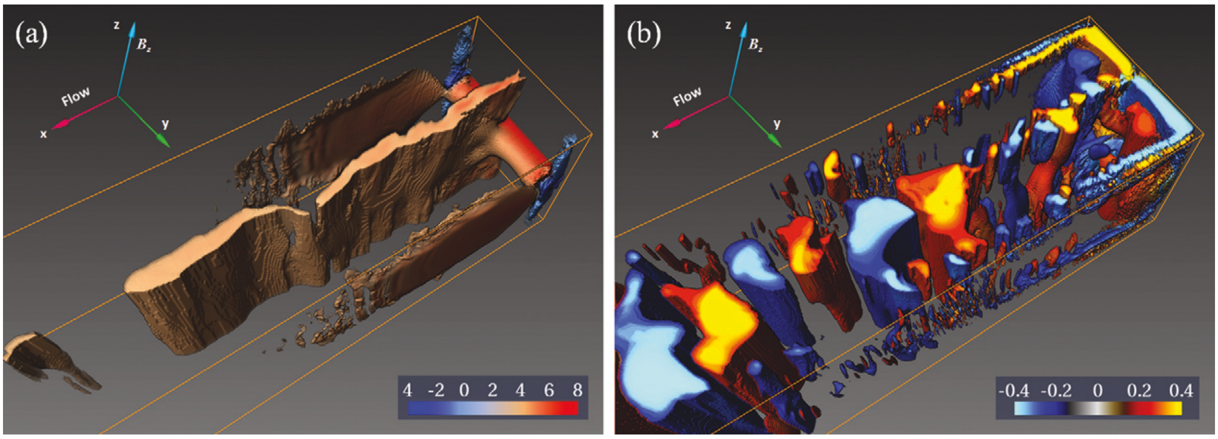

Fig. 2: Transformation of the inlet jet and development of Q2D state. The streamwise (a) and spanwise (b) velocity components u_x and u_y are shown in the entry region $0 < x < 4$ of the developed state at $t = 20$. The velocity magnitude contours at ranges $u_x = -1 \ldots 2$ (a) and $u_y = -0.2 \ldots 0.2$ (b) are blanked for better visibility.

the classical Gauss-Lobatto version because it provides better resolution in the duct's core, which is necessary in our case to accurately reproduce the jet's transformation. Similar coordinate transformations were used in our prior studies of MHD flows with jets [21,22].

One complete simulation of the flow at $Re = 20000$ and $Ha = 1000$ is performed. As we will see below, these values correspond to a regime with a spectacular jet transformation. They are also interesting as belonging to the range of the highest values of Re and Ha achievable at the existing experimental facilities [17]. The simulation starts with the jet initiated at the inlet of a quiescent duct and continues for 40 non-dimensional time units. The last 20 units are considered to be corresponding to a fully developed flow and used for collection of turbulent statistics.

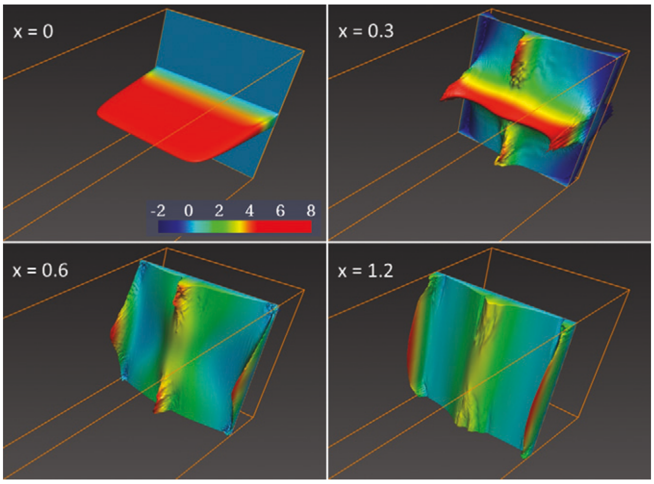

Fig. 3: Transformation of the streamwise velocity profile in the inlet region. Distributions of u_x in (y, z) cross-sections at several x-positions in the range $x = 0 \ldots 1.2$ are shown. The flow state is the same as in figs. 2 and 4(c).

Results. – The main features of the initial transformation of the inlet jet are illustrated in figs. 2 and 3. We see that the inlet velocity profile, with its strong gradients along the magnetic field lines is rapidly suppressed and disappears completely a short distance downstream. Figure 3 shows that the profile is already changed significantly at $x = 0.3$. Three planar jets oriented along the magnetic field lines appear: two near the sidewalls and one in the middle of the duct. The streamwise flux is increasingly concentrated in these jets. Practically no traces of the inlet profile are visible at $x = 1.2$, *i.e.*, at the distance of just 0.6 of the duct width from the inlet. The flow acquires Q2D form, with the planar jets extending between the Hartmann walls and having very weak velocity gradients along the field lines outside of the Hartmann boundary layers.

The formation of the two sidewall jets is not surprising. Similar structures are commonly observed in wall-bounded parallel flows entering a zone of a strong transverse magnetic field or, as in our case, flows experiencing a sudden expansion and, thus, a sudden increase of Ha. A detailed explanation can be found, *e.g.*, in [2,18]. The reason is the spanwise (normal to the flow and the magnetic field) electric currents that appear upon the entry or expansion. The interaction between the currents and the magnetic field produces the Lorentz force in the negative x-direction, *i.e.*, the force braking the streamwise flow. Since the electric currents have to close within the fluid, the strength of their spanwise component decreases to zero in the sidewall boundary layers. The respective drop of the Lorentz force leads to redistribution of the streamwise velocity into the so-called M-shaped profile, in which most of the streamwise flux is carried by planar sidewall jets. The thickness of the jets scales as $\sim Ha^{-1/2}$.

The surprising new feature of our flow is the strong (with the maximum streamwise velocity and cumulative flux comparable to those of the sidewall jets) third planar jet located in the middle of the duct. We explain this

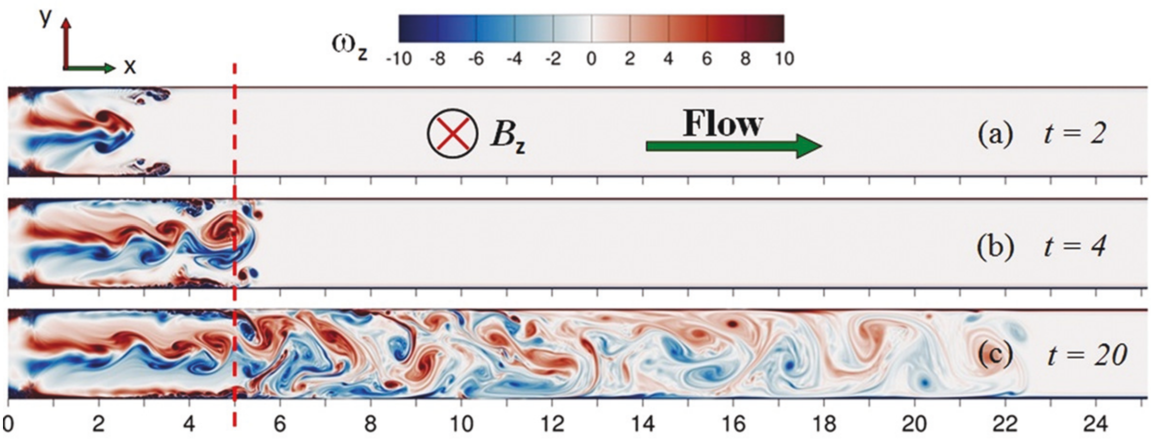

Fig. 4: Spatio-temporal evolution of the flow shown in the cross-section at $z = 0$. Distributions of the vorticity component ω_z parallel to the applied magnetic field are plotted for two instants of the transient stage of flow development ((a) and (b)) and for the nearly fully developed flow stage (c). The red dashed line indicates the position $x \approx 5$, where the three-jet structure starts to break down and the flow forms a street of Q2D vortices. See supplementary videos (SM) for further information.

phenomenon by the very high value $Ha = 1000$, which is substantially higher than the values achieved in earlier studies. The sidewall jets are very thin and, therefore, experience strong hydrodynamic resistance, which does not allow them to carry the flux corresponding to $Re = 20000$. The central jet appears as a response to that.

The next step of the flow development is the instability of the jets and formation of Q2D vortices (see fig. 2(b)). The only plausible explanation is the Kelvin-Helmholtz instability caused by strong shear and inflection points in the velocity profiles of the jets. The instability is triggered by the strong perturbations remaining from the flow rearrangement near the inlet and further enhanced by the interaction between the three unstable jets. The resulting growth of the perturbations is very rapid. Visible breakdown of the jets and formation of vortices occur at $x \approx 5$. The state of the flow downstream of this location can be characterized as decay of Q2D wall-bounded turbulence.

The nearly two-dimensional nature of the flow outside the inlet region (approximately at $x > 1.2$) means that it can be illustrated by 2D distributions of variables in a cross-section perpendicular to the magnetic field. As an example, the field-parallel vorticity component ω_z in the mid-plane $z = 0$ is shown in fig. 4. To facilitate better understanding of the flow evolution, two snapshots of the transient stage (at $t = 2$ and $t = 4$) are shown in addition to the fully developed stage at $t = 20$. Further illustrations can be found in the animations of the distributions of ω_z and u_x in the plane $z = 0$ posted as supplementary videos `suppl1_Omegaz_xy.mp4` and `suppl2_ux_xy.mp4` (spatio-temporal flow evolution shown by the vertical vorticity ω_z and streamwise velocity u_x) (SM). The animations cover the entire computed evolution of the flow including the transient stage $0 < t < 20$ and the fully developed stage $20 < t < 40$.

We now report the results of the quantitative analysis of the time-averaged flow properties: mean velocity and turbulence statistics. y-distributions in the duct's mid-plane $z = 0$ are shown in fig. 5 for several x-locations. As one can see in fig. 5(a), a flat jet entering the duct at $x = 0$, already undergoes strong deformation at $x = 0.3$, so that the streamwise velocity decreases by a factor of two. At the same time, the jet-like side layers and return flows are formed near the walls parallel to the magnetic field (see fig. 3, $x = 0.3$). At $x = 0.6$, the velocity on the axis drops significantly, which is accompanied by restructuring of the entire flow pattern. We see pronounced sidewall layers and formation of a central jet. Further growth and stabilization of this structure is observed at $x = 1.2$ (see also fig. 3) and $x = 3$. An important feature clearly seen in the plots is that the central jet is much wider than the sidewall jets and, evidently, carries a larger portion of the streamwise flux. A short distance downstream, at $x = 4$, we already see modification of the velocity profile related to the instability and interaction between the jets. Further downstream, at $x = 6$, the jets practically disappear (see also fig. 4) and the mean velocity profile has the shape largely determined by the strong mixing by Q2D vortices, although weak traces of the three-jet pattern remain. The shape is retained further downstream, as one can see in the profiles at $x = 8$ and $x = 16$.

The inflection points of the mean velocity profile can be identified by the extrema of the gradient $\partial\langle u_x\rangle/\partial y$, which are clearly visible at $x \leq 6$ in fig. 5(b). The maxima of the root-mean square (rms) turbulent streamwise fluctuations $\langle u_x'^2\rangle^{1/2}$ are found at the same points. In the vicinity of these points the energy is transferred to perturbations from the mean flow through the streamwise component $\langle u_x'^2\rangle^{1/2}$. After that, the energy is redistributed among other components. Accordingly, the maximum $\langle u_y'^2\rangle^{1/2}$ occupies a position on the jet axis (see fig. 5(d)).

The main component $\langle u_x' u_y'\rangle$ of shear turbulent stress is shown in fig. 5(e). In the upstream portion of the duct, where the three planar jets are present, *i.e.*, approximately

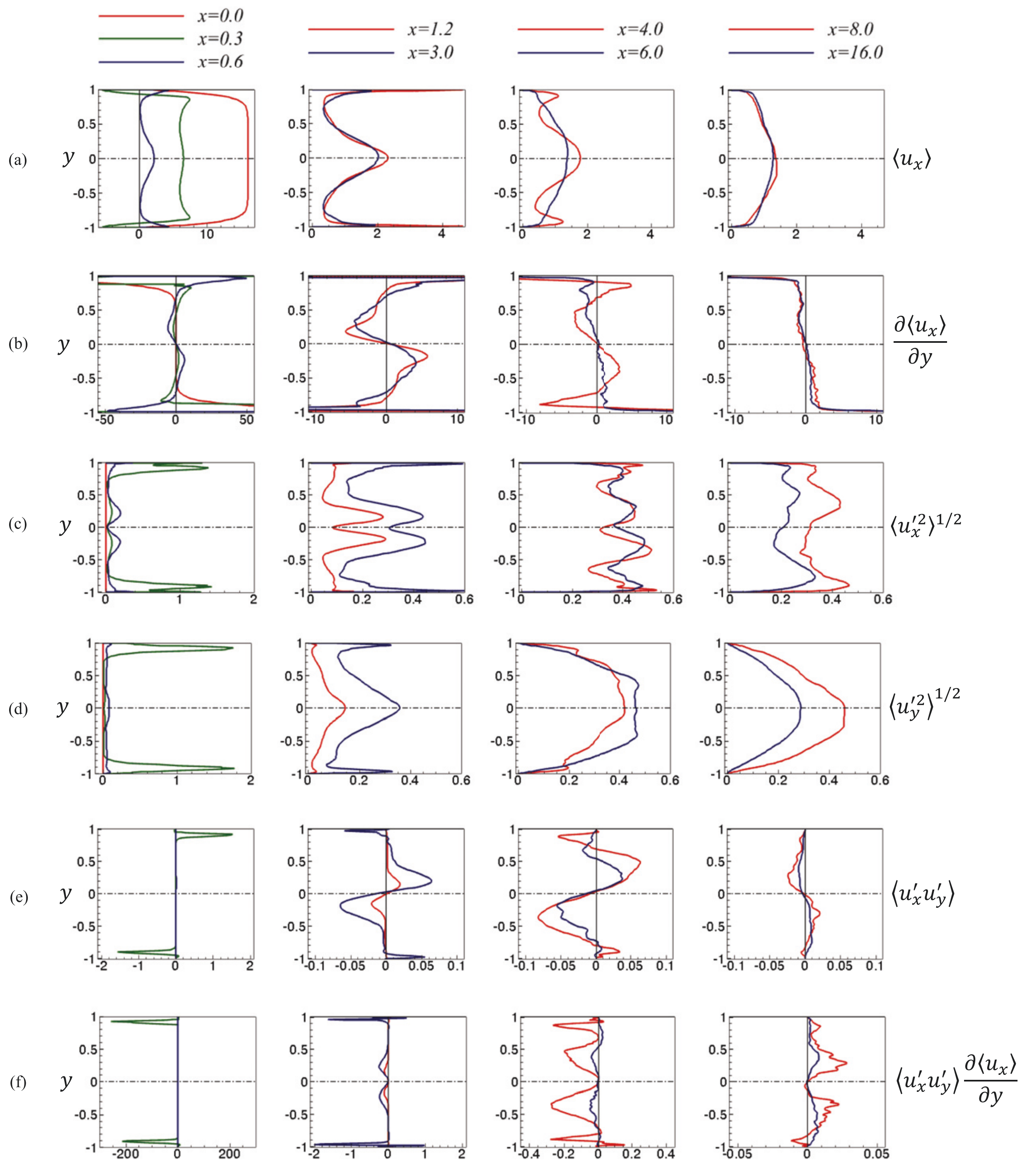

Fig. 5: Profiles of time-averaged statistical properties plotted as functions of the spanwise coordinate y at $z = 0$ (in the mid-plane of the duct). Data for several cross-sections $x = \text{const}$ corresponding to distinct stages of flow evolution are shown. The plots are generated from the velocity fields, in which values at every fourth point in each direction are stored. (a) and (b) mean streamwise velocity $\langle u_x \rangle$ and its gradient $\partial \langle u_x \rangle / \partial y$; (c) and (d) rms velocity fluctuations $\langle u_x'^2 \rangle$ and $\langle u_y'^2 \rangle$; (e) turbulent shear stress in the plane perpendicular to the magnetic field $\langle u_x' u_y' \rangle$; (f) turbulence production in the plane perpendicular to the magnetic field $\langle u_x' u_y' \rangle \partial \langle u_x \rangle / \partial y$.

at $x \leq 4$, we see the sharp local maxima corresponding to the maxima of the rms fluctuations and the inflection points. At approximately $x > 8$, the sign of $\langle u_x' u_y' \rangle$ is reversed in comparison to the respective values at $x < 8$. This is related to the change in the profiles of the turbulence production rate $\langle u_x' u_y' \rangle \partial \langle u_x \rangle / \partial y$. We see in fig. 5(f) that in the range $1.2 \leq x \leq 6$, direct energy transfer from the mean flow to the perturbations takes place. However,

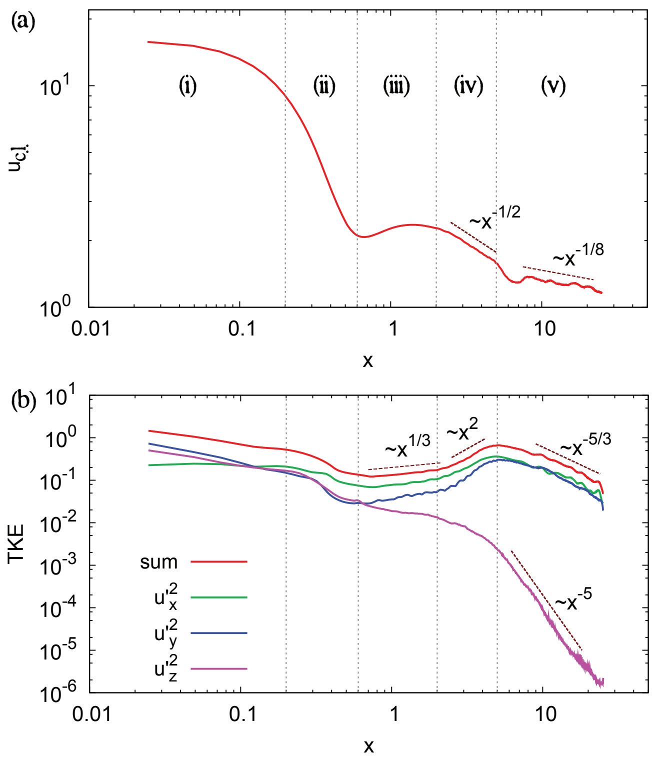

Fig. 6: Spatial distribution of the time-averaged center-line velocity $u_{c.l.}$ (a) and turbulent kinetic energy (b). The values of TKE are averaged over (y,z) cross-sections.

at $x \geq 8$ the value $\langle u'_x u'_y \rangle \partial \langle u_x \rangle / \partial y$ changes its sign, which indicates the energy transfer from the 2D perturbations generated upstream back to the mean flow, *i.e.*, the effect of negative turbulent viscosity typical for 2D free shear flows. A similar effect was found in the experiments [3] with the magnetic field oriented along the plane of the jet. Analysis of the statistical properties at other values of x (not shown) demonstrates existence of a transitional region approximately at $6 < x < 8$, where the processes of turbulence generation by the mean flow and the energy transfer from the perturbations into the mean flow coexist. In this range, the turbulent momentum flux $\langle u'_x u'_y \rangle$ changes sign several times.

We continue with the analysis of the time-averaged centre-line velocity $u_{c.l.}$ and kinetic energy of velocity fluctuations averaged over time and the (y,z) cross-sections. The evolution of these properties along the duct shown in fig. 6 allows us to identify five zones of distinct flow behaviour.

In zone (i), which is located immediately next to the inlet, the flat jet initially oriented orthogonally to the magnetic field is decelerated by the Lorentz force (see fig. 6(a)). At the same time, due to the z-component of the curl of the Lorentz force $-(Ha^2/Re)\partial j_x/\partial x$, which has opposite signs on both sides of the axis, lateral shear layers are formed at the walls parallel to the field. The three-dimensional fluctuations created during this stage are predominantly in the transverse velocity components u'_y and u'_z (see fig. 6(b)). They lose their energy to the Joule dissipation as they move downstream.

Zone (ii) corresponds to further development of the sidewall layers, in which the fluid is accelerated since the local x-component of the Lorentz force is nearly zero there. Correspondingly, $u_{c.l.}$ continues to drop and the central jet starts to form (see fig. 3). A fast drop of the fluctuation energy is observed. We see in fig. 6(b) that the fluctuations of the streamwise velocity u'_x become significantly stronger than u'_y and u'_z evidently as a manifestation of formation of the sidewall and central planar jets.

In zone (iii), there is an increase of the axial velocity due to the final formation of the central jet (see fig. 6(a)). The growth of the 3-jet pattern causes a visible growth (with the slope approaching $\sim x^{1/3}$) of the fluctuation energy in u'_x and u'_y. Figure 4(c) and the supplementary videos (SM) lead us to the conclusion that this growth is a manifestation of the beginning instability of the jet. Also in this zone, the flow's transformation into an anisotropic state causes decay of the field-parallel fluctuation component u'_z.

The three planar jets disintegrate into vortices in zone (iv). This is associated with rapid increase (with the slope about $\sim x^2$) of the kinetic energy in u'_x and u'_y and decrease (at about $\sim x^{-1/2}$) of the centre-line velocity. The amplitude of u'_z continues to decrease as the flow becomes increasingly anisotropic.

Zone (v) is that of decaying Q2D turbulence. Due to the Q2D nature of the flow, the effect of magnetic suppression is weak, and the decay is predominantly caused by viscosity, which acts in the shear layers between the vortices as well as in the sidewall and Hartmann boundary layers. The process is characterized by slow ($\sim x^{-1/8}$) decrease of $u_{c.l.}$, very fast ($\sim x^{-5}$) suppression of u'_z, and the decay of the velocity fluctuations u'_x and u'_y corresponding to the Q2D vortices with the rate approaching $\sim x^{-5/3}$. Interestingly, the latter is consistent with the findings of [22], where a close decay rate $\sim x^{-1.7}$ was reported for Q2D vortices generated by inlet honeycomb in a duct with strong transverse magnetic field.

Summary and outlook. – We have presented results of a numerical simulation of a flat jet expanding into a square duct with a transverse magnetic field. The previously unexplored case of large expansion ratio and high Re and Ha is considered. It is found that the inlet velocity distribution is rapidly suppressed, and the flow acquires a non-trivial structure, which, in addition to the anticipated sidewall jets of a classical MHD M-shaped profile, includes a strong central jet oriented parallel to the field lines. The jets experience the Kelvin-Helmholtz instability, which leads to their noticeable distortion and complete breakdown at the distance, respectively, ∼1 and 2–3 duct widths from the inlet. Further downstream, the flow is represented by a street of slowly decaying high-amplitude Q2D vortices. The flow regime with three jets is entirely new. In hindsight, it is indicated by the classical experiment [1]. The existence of the regime has, however, not been demonstrated or even explicitly predicted previously.

The new flow regime will be further explored in our numerical and experimental studies. At this moment, we can plausibly assume its existence in a broad range of *Re* and *Ha*, with the quantitative characteristics affected by these parameters as well as by the flow geometry (the expansion ratio and the aspect ratio of the duct).

It is interesting to compare the flow with its counterparts based on different inlet conditions, such as a round jet, a flat jet in the plane of the magnetic field, or a honeycomb. At a sufficiently strong MHD effect, the ultimate far-downstream state of all these flow is qualitatively the same, *i.e.*, Q2D turbulence dominated by large vortices. The path of transition to this state and, as a result, its characteristics are, however, expected to vary strongly with the inlet conditions. Leaving a thorough investigation of these questions to future studies, we mention that the configuration considered in this paper presents a very robust mechanism of generation of Q2D turbulence. The flow does not show a tendency to asymmetric states with the flow rate shifted toward one of the sidewalls or high-amplitude fluctuations between such states, which are known phenomena for non-MHD jets and, as indicated by our preliminary research, flat jets parallel to the magnetic field. The strong shear between the three jets, well-developed inflection points, and high-amplitude perturbations resulting from the flow transformation in the inlet area assure strong instability and rapid development of Q2D turbulence with repeatable properties and low sensitivity to such factors as noise at the inlet or imperfections of an experimental setup.

The new robust mechanism of generation of Q2D turbulence opens possibilities of detailed studies of its properties including validation of theoretical models, such as [7,11,23–27]. It also has practical importance. Generation of strong and slowly decaying Q2D vortices is associated with substantial, possibly orders-of-magnitude increase of the rates of heat, admixture, and momentum transfer [28], which is of critical significance for design and operation of liquid metal blankets of nuclear fusion reactors.

* * *

The authors acknowledge the RSF research grant 20-69-46067. DK is supported by the DFG research project KR 4445/2-1 within a joint Russian-German collaboration program. OZ is supported by the US NSF (grant No. CBET 1803730). The simulations have been performed at the SuperMUC-NG cluster at the Leibniz Rechenzentrum Garching (Large Scale Project pn68ni of the Gauss Centre for Supercomputing), the visualizations were performed at the Computer Center of TU Ilmenau.

REFERENCES

[1] Branover G. G. and Shcherbinin E. V., *Magnetohydrodynamics*, **2** (1966) 55.

[2] Walker J. S., Ludford G. S. S. and Hunt J. C. R., *J. Fluid Mech.*, **56** (1972) 121.

[3] Votsish A. D. and Kolesnikov Y. B., *Magnetohydrodynamics*, **12** (1976) 422.

[4] Davidson P. A., *J. Fluid Mech.*, **299** (1995) 153.

[5] Davidson P. A., *Introduction to Magnetohydrodynamics* (Cambridge University Press) 2016.

[6] Zikanov O. and Thess A., *J. Fluid Mech.*, **358** (1998) 299.

[7] Thess A. and Zikanov O., *J. Fluid Mech.*, **579** (2007) 383.

[8] Zikanov O., Krasnov D., Boeck T., Thess A. and Rossi M., *ASME Appl. Mech. Rev.*, **66** (2014) 030802.

[9] Krasnov D. S., Zikanov O. and Boeck T., *J. Fluid Mech.*, **704** (2012) 421.

[10] Zikanov O., Krasnov D., Boeck T. and Sukoriansky S., *J. Fluid Mech.*, **867** (2019) 661.

[11] Verma M. K., *Rep. Progr. Phys.*, **80** (2017) 087001.

[12] Harada H., Okazawa K., Tanaka M. and Takeuchi E., *Proceedings of the International Symposium on Electromagnetic Processing of Materials, Nagoya, Japan, October 1994*.

[13] Kim J., Park J. and Choi H., *Large eddy simulation of magnetic dumping of jet*, *Proceedings of the XXI ICTAM Conference* (ICTAM, Warsaw, Poland) 2004.

[14] Bühler L., Horanyi S. and Arbogast E., *Fusion Eng. Design*, **82** (2007) 2239.

[15] Bühler L., *Fusion Sci. Technol.*, **52** (2007) 595.

[16] Mistrangelo C., *J. Fluid Mech.*, **674** (2011) 132.

[17] Pyatnitskaya N., Luchinkin N., Belyaev I., Kolesnikov Y., Krasnov D., Listratov Y., Zikanov O. and Sviridov E., *J. Phys.: Conf. Ser.*, **1689** (2020) 012002.

[18] Müller U. and Bühler L., *Magnetohydrodynamics in Channels and Containers* (Springer) 2001.

[19] Krasnov D., Zikanov O. and Boeck T., *Comput. Fluids*, **50** (2011) 46.

[20] Zhao Y. and Zikanov O., *J. Fluid Mech.*, **692** (2012) 288.

[21] Belyaev I., Krasnov D., Kolesnikov Y., Biryukov D., Chernysh D., Zikanov O. and Listratov Y., *Phys. Fluids*, **32** (2020) 094106.

[22] Zikanov O., Krasnov D., Boeck T. and Sukoriansky S., *J. Fluid Mech.*, **867** (2019) 661.

[23] Davidson P., *J. Fluid Mech.*, **336** (1997) 123.

[24] Pothérat A., Sommeria J. and Moreau R., *J. Fluid Mech.*, **424** (2000) 75.

[25] Pothérat A. and Kornet K., *J. Fluid Mech.*, **783** (2015) 605.

[26] Burattini P., Zikanov O. and Knaepen B., *J. Fluid Mech.*, **657** (2010) 502.

[27] Verma M. K., Alam S. and Chatterjee S., *Phys. Plasmas*, **27** (2020) 052301.

[28] Kolesnikov Y. B. and Tsinober A. B., *Fluid Dyn.*, **9** (1974) 621.